Human Cancer Biology

Clinical Cancer Research

Expression Profiles and Clinical Correlations of Degradome Components in the Tumor Microenvironment of Head and Neck Squamous Cell Carcinoma

Angela Stokes[1], Juho Joutsa[6,7,8,9], Risto Ala-aho[6,8], Mark Pitchers[1], Caroline J. Pennington[1], Craig Martin[2], Don J. Premachandra[3], Yasunori Okada[10], Juha Peltonen[4], Reidar Grénman[5,7], Helen A. James[1], Dylan R. Edwards[1], and Veli-Matti Kähäri[6,7,8]

Abstract

Purpose: Head and neck squamous cell carcinomas (HNSCC) are characterized by high morbidity and mortality, largely due to the high invasive and metastatic potential of these tumors, high recurrence rates, and low treatment responses. Proteinases have been implicated in several aspects of tumor growth and metastasis in a broad range of tumors including HNSCC.

Experimental Design: Comprehensive expression profiling of proteinases [matrix metalloproteinases (MMPs), A disintegrin and metalloproteinase (ADAMs), and ADAMs with thrombospondin motif (ADAMTSs)] and their inhibitors [tissue inhibitor of metalloproteinases (TIMPs)] was done using quantitative real-time reverse transcription-PCR analysis of a large cohort of tissue samples representing the tumor ($n = 83$), the invasive margin ($n = 41$), and the adjacent tissue ($n = 41$) from 83 HNSCC patients, along with normal tissue controls ($n = 13$), as well as cell lines established from tumors of 34 HNSCC patients.

Results: The results show specifically elevated gene expression of several proteinases, including MMP1, MMP3, MMP10, and MMP13 within tumor tissue and peritumoral adjacent tissue. In addition, the results identify several novel HNSCC-associated proteinases, including *ADAM8*, *ADAM9*, *ADAM17*, *ADAM28*, *ADAMTS1*, *ADAMTS8*, and *ADAMTS15*. There were also significant differences in proteinase expression based on clinical parameters, i.e., tumor location, grade, and local invasion. *MMP13* expression was significantly higher in large (>4 cm) locally invasive tumors ($P < 0.05$). *MMP9* expression was significantly decreased in tumors with regional metastasis, whereas increased expression of *ADAM8* was noted in the metastatic tumors ($P < 0.001$ for both).

Conclusions: These findings suggest the HNSCC degradome as a valuable source of diagnostic, predictive, and prognostic molecular markers for these malignant tumors. *Clin Cancer Res; 16(7); 2022–35.* ©*2010 AACR.*

Head and neck squamous cell carcinoma (HNSCC) can be defined as a malignant tumor derived from the squamous epithelial cells that line the upper aerodigestive tract, which extends from the surface of the lips to the cervical surface of the esophagus. HNSCC is the fifth most common cancer worldwide and, in 2002, was the cause of over 300,000 deaths worldwide (1). The overall survival rates of HNSCC patients (~50%) have remained unaltered for over 20 years. The presence of lymph node metastases is the single most important predictive factor for HNSCC patients resulting in a 50% decrease in survival (2, 3).

The degradome comprises both the complete set of proteases (also known as peptidases and proteinases) expressed by a cell, tissue, or organism at a given time, and the substrate repertoire of a given proteinase (4). There is a well-established association between matrix proteolysis and cancer invasion and metastasis, and the proteinases of every class have been linked to malignancy and invasion of tumor cells (5). However, through the study of transgenic models and the identification of further proteinases and proteinase substrates, it is now clear that the proteinases also play crucial roles in early tumorigenic

Authors' Affiliations: [1]Biomedical Research Centre, University of East Anglia; [2]Department of Oncology, Norfolk and Norwich University Hospital NHS Trust; and [3]ENT Department, Norfolk and Norwich University Hospital NHS Trust, Norwich, United Kingdom; Departments of [4]Anatomy and Cell Biology, [5]Otorhinolaryngology-Head and Neck Surgery, [6]Dermatology, and [7]Medical Biochemistry and Genetics, and [8]MediCity Research Laboratory, University of Turku and Turku University Hospital; and [9]Turku Graduate School of Biomedical Sciences, Turku, Finland; [10]Department of Pathology, School of Medicine, Keio University, Tokyo, Japan

Note: Current address for A. Stokes: Department of Oral Pathology, Kings College London Dental Institute, UK.

A. Stokes and J. Joutsa contributed equally to this work.

Corresponding Author: Veli-Matti Kähäri, Department of Dermatology, University of Turku, P.O.B. 52, Turku FI-20521, Finland. Phone: 358-2-3131600; Fax: 011-358-2-3131610; E-mail: veli-matti.kahari@utu.fi.

doi: 10.1158/1078-0432.CCR-09-2525

Translational Relevance

This study provides novel information on the proteinases and their inhibitors participating in the progression of head and neck squamous cell carcinomas (HNSCC). The study cohort is exceptionally large, enabling us to evaluate the results in the light of previous findings in the field. In addition, several HNSCC-associated degradome components presented for the first time in this study serve as a valuable source of novel diagnostic, predictive, and prognostic factors, as well as follow-up markers for the early detection of metastases and efficacy of therapy. Furthermore, these degradome components provide potential targets for novel treatment modalities in HNSCC patients.

events such as angiogenesis, apoptosis, cell dissociation, and cell migration (6). In addition to their recognized roles in extracellular matrix degradation, secreted proteinases also play important roles in controlling the bioactivity of cytokines and growth factors and in the shedding of cell surface growth factors and adhesion receptors (7, 8). Thus, proteinases have complex influences on the tumor microenvironment and there is growing evidence that many proteinases can act in an antitumorigenic fashion in addition to their classic proinvasive and prometastastic roles (9).

Matrix metalloproteinases (MMPs) are a zinc-dependent metalloproteinase subfamily consisting of 23 members that can collectively degrade all major components of the extracellular matrix (10). Most MMPs are secreted; however, the membrane-type MMPs contain either a transmembrane domain or glycosylphosphatidylinositol anchor locating them to the cell surface. The main inhibitors of MMP activity are tissue inhibitors of the metalloproteinases (TIMPs), a group of four secreted proteins that reversibly bind and inactivate MMPs in a 1:1 stoichiometric manner (11). TIMPs differ in their expression patterns and inhibitory activities toward certain MMPs (11). Moreover, TIMP2 can also be secreted in a complex with proMMP2 and function in MMP2 activation (12).

The A disintegrin and metalloproteinases (ADAMs) are a group of 21 human transmembrane metalloproteinases that belong to the same family of zinc proteinases as the MMPs and which contain a unique integrin receptor–binding disintegrin domain (8). All ADAMs are not catalytically active, as only approximately half contain the conserved catalytic-site consensus motif (HEXXH) in their metalloproteinase domain (7). The ADAMs with thrombospondin motifs (ADAMTSs) is a group of 19 secreted metalloproteinases, which are close relatives of the ADAMs. Instead of the transmembrane domains and cytoplasmic tails of the ADAMs, the ADAMTSs contain a variable number of thrombospondin-like motifs (13, 14). The TIMPs also inhibit the activity of selected ADAM and ADAMTS members (15–17).

Thus far, several studies have explored proteinase involvement in HNSCC, mainly using immunohistochemical methods to measure the presence of MMPs in tissue sections. Indeed, most proteinases studied and implicated in HNSCC are increased in expression in tumor tissues and metastases, and are therefore linked to HNSCC progression at some level in at least one study. However, the observations are often contradictory and thus the exact role of these factors in HNSCC pathology remains unclear. There are many reasons for this; for instance, diverse techniques, the lack of reliable antibodies for many proteinases, the low patient numbers, and the pooling of tumors from different sites. It is consensus that MMP2, 7, 9, 10, 13, and TIMP1 are particularly involved in HNSCC pathogenesis and progression (18–20). There are further suggestions of the involvement of MMP1, 3, 11, 14, and TIMP2, but no other MMPs or TIMPs have been studied (18–20). In contrast, the ADAM and ADAMTS families have not been extensively studied in this tumor type. There is evidence for their involvement in HNSCC as both ADAM10 (21) and ADAM12 (22) are overexpressed in oral HNSCCs.

In this study, we have investigated the expression of the entire MMP and TIMP families, and subsets of the ADAMs and ADAMTSs in a large cohort of tumor samples of HNSCC patients and cell lines established from these tumors. These data provide a descriptive degradome of HNSCC tissues and identify several novel proteinases, which can serve as molecular markers for the classification and prognosis of this malignant tumor.

Materials and Methods

Tissue samples and cDNA preparation. This study received approval from the Norwich Local Research Ethics Committee, the Norwich and Waveney Research Governance Committee, and the Partners in Cancer Research Tissue Bank Committee. Studies at the University of Turku were approved by the Joint Ethical Committee of the University of Turku and Turku University Hospital. Participants gave their informed consent and the study was conducted according to the declaration of Helsinki.

Forty-one HNSCC tissue samples sets (each containing of adjacent, margin, and center tumor tissues) were obtained from the Norfolk and Norwich University Hospital Tissue Bank. Detailed procedures for obtaining informed patient consent, sample collection, processing and storage, and finally, collection of relevant clinical information has already been described (23). Forty-two HNSCC center tumor samples were obtained from surgically removed tumors in Turku University Hospital between years 2003 and 2005 from both genders (ranging in age from 39-86 y). The clinical parameters corresponding to the tumors are shown in Table 1. As a control, 13 normal nonneoplastic tissue samples of uvular, tonsil, and soft palate mucosa of patients were obtained during tonsillectomy or surgery for sleep apnea in Turku University Hospital. Total RNA was isolated

from the tissue samples by homogenizing in RNA bee (Biogenesis Ltd) using the Qiagen TissueLyser (Qiagen) and then the SV Total RNA isolation kit or RNA Easy Mini kit (Promega) as previously described (24, 25) or using the acid-guanidium thiocyanate-phenol-chloroform method (26). RNA quality and concentration was then determined using the NanoDrop ND-1000 UV-Vis Spectrophotometer (Labtech). Total RNA (1 μg) was reverse transcribed with 2 μg random hexamers (Amersham Pharmacia Biotech) and 200 units of SuperScript II reverse transcriptase (Invitrogen) according to the manufacturer's instructions using a GRI DNA Engine (GRI). The cDNA was diluted 1:100 with PCR grade water and stored at −20°C.

Cell cultures. Human HNSCC cell lines (n = 34) were established at the time of operation from HNSCCs (27). The clinical data of the corresponding tumors are shown in Table 1. Cells were cultured in DMEM supplemented with 6 nmol/L glutamine, nonessential amino acids, and 10% FCS. Normal human epidermal keratinocytes (NHEK-PC) were purchased from PromoCell and other primary NHEKs (n = 8) were established from skin samples, and cultured in Keratinocyte Basal Medium 2, supplemented with SingleQuots (Cambrex Bioscience), as previously described (28). Total RNA was extracted from cultured cells using the Trizol reagent (Invitrogen) and cDNA was synthesized as above.

Quantitative real-time PCR. For qPCRs, specific primers and probes for all human MMPs, TIMPs, catalytically active ADAMs, and some ADAMTSs were designed as previously described (Table 2; refs. 24, 25, 29). The 18S rRNA was used as an endogenous control to normalize for differences in the amount of total RNA in each sample, using previously validated procedures (30). PCRs were done as previously described (29) using the ABI 7700 real-time PCR machine (Applied Biosystems) with each reaction containing 5 ng of reverse-transcribed RNA (1 ng for 18S) in a 25-μL reaction. The relative RNA levels in each sample were determined by performing standard curves for all target genes covering 1 to 0.0625 ng of RNA for 18S and 20 to 0.5 ng RNA for all other genes.

Protein extraction and quantification. Frozen tissue samples were homogenized in ice-cold protein extraction buffer (pH 6.7) containing 500 mmol/L Tris (Melford Laboratories Ltd), 200 mmol/L M NaCl (Sigma-Aldrich), 10 mmol/L $CaCl_2$ (Sigma-Aldrich), 1% (v/v) Triton X-100 (BDH), and 1 complete, Mini, EDTA-free proteinase inhibitor cocktail tablet (Roche Diagnostics Ltd) per 10 mL. Samples were then placed on ice for 1 h, before centrifugation at 6,000 rpm for 1 min. The resultant protein containing supernatant was then stored at −20°C. The protein content for each sample was quantified using the BCA protein assay kit (Perbio Scientific UK Ltd). However, due to the high Triton X-100 content of the protein extraction buffer, the samples required dilution in PBS at least 1:10.

Zymography. For gelatin zymography, 10 μg of protein, per sample, were run under nonreducing conditions at 30 mA on a 10% SDS-polyacrylamide gel copolymerized with 1 mg mL^{-1} of gelatin (Sigma-Aldrich) in TGS running buffer (Bio-Rad Laboratories Ltd). A positive control (for MMP2 and MMP9) of conditioned medium from baby hamster kidney cells stably transfected with the human *MMP9* gene was used. The gel was then washed overnight in rinse buffer containing 50 mmol/L Tris-HCl (pH 7.8), 5 mmol/L $CaCl_2$, and 2.5% (w/v) Triton X-100. The gel was then incubated for 18 h in incubation buffer containing 50 mmol/L Tris-HCl (pH 7.8) and 5 mmol/L $CaCl_2$ at 37°C. Proteolytic activity was then visualized as a clear band on a blue background by staining with Coomassie blue stain containing 10% (v/v) acetic acid, 30% (v/v) isopropanol (Fisher-Scientific), and 2.5 mg/mL Coomassie blue (Bio-Rad Laboratories Ltd) for 1 h and then destaining in 10% (v/v) acetic acid and 30% (v/v) isopropanol for 1 h.

Western blotting. Reduced protein samples (10 μg per lane) were loaded onto a 10% polyacrylamide gel and ran at 30 mA in TGS running buffer. A Precision Plus Protein dual-color standard (Bio-Rad Laboratories Ltd) was

Table 1. The clinical data corresponding to the HNSCC tumor samples and cell lines

Clinical features of the HNSCC tumors		
Characteristic	**Tumors, *n* (%)**	**Cell lines, *n* (%)**
Tumor location		
Oral cavity	39 (47)	16 (47)
Pharynx	11 (13)	1 (3)
Larynx	14 (17)	11 (32)
Other primary	2 (2)	0 (0)
Lymph node metastasis	17 (21)	6 (18)
Histologic grading		
Well differentiated (G1)	26 (31)	12 (35)
Moderately differentiated (G2)	31 (38)	14 (41)
Poorly differentiated (G3)	24 (29)	8 (24)
Unknown	2 (2)	0 (0)
T classification		
T1	15 (18)	4 (12)
T2	27 (33)	14 (41)
T3	16 (19)	6 (18)
T4	14 (17)	9 (26)
Unknown	11 (13)	1 (3)
Lymph node involvement		
Positive	38 (46)	15 (44)
Negative	37 (44)	19 (56)
Unknown	8 (10)	0 (0)

NOTE: The clinicopathologic features of HNSCC tumors used for analysis of tissue samples and establishment of cell lines with respect to location of the primary tumor, histologic grading, size, and lymph node metastasis.

Table 2. Primers and probes used for quantitative Real-time RT-PCR

MMP-1	Forward primer	5′-AAGATGAAACGTGGACCAACAATT –3′
	Reverse primer	5′-CCAAGAGAATGGAAGAGTTC –3′
	Probe	5′-FAM-CAGAGAGTACAACTTACATCGTGTTGCGGCTC-TAMRA –3′
MMP-2	Forward primer	5′-AACTACGATGACGACCGCAAGT –3′
	Reverse primer	5′-AGGTCTAAATGGGTGCCATCA –3′
	Probe	5′-FAM-CTTCTGGCCTGACCAAGGGTACAGCC-TAMRA –3′
MMP-3	Forward primer	5′-TTCCGCCTGTCTCAAGATGATAT –3′
	Reverse primer	5′-AAAGGACAAAGCAGGATCACAGTT –3′
	Probe	5′-FAM-TCAGTCCCTCTATGGACCTCCCCCTGAC-TAMRA –3′
MMP-7	Forward primer	5′-CTTTGCGCGAGGAGCTCA –3′
	Reverse primer	5′-CAGGCGCAAAGGCATGA 3′
	Probe	5′-FAM-CCATTTGATGGGCCAGGAAACACG-TAMRA –3′
MMP-8	Forward primer	5′-CACTCCCTCAAGATGACATCGA 3′
	Reverse primer	5′-ACGGAGTGTGGTGATAGCATCA 3′
	Probe	5′-FAM-CAAGCAACCCTATCCAACCTACTGGACCAA-TAMRA –3′
MMP-9	Forward primer	5′-AGGCGCTCATGTACCCTATGTAC –3′
	Reverse primer	5′-GCCCGTGGCTCAGGTTCA –3′
	Probe	5′-FAM-CATCCGGCACCTCTATGGTCCTCG-TAMRA –3′
MMP-10	Forward primer	5′-GGACCTGGGCTTTATGGAGATAT –3′
	Reverse primer	5′-CCCAGGGAGTGGCCAAGT –3′
	Probe	5′-FAM-CATCAGGCACCAATTTATTCCTCGTTGCT-TAMRA –3′
MMP-11	Forward primer	5′-GGGTGCCCTCTGAGTCGA –3′
	Reverse primer	5′-TCACAGGGTCAAACTTCCAGTAGA –3′
	Probe	5′-FAM-ATGCTGATGGCTATGCCTACTTCCTGCG-TAMRA –3′
MMP-12	Forward primer	5′-CGCCTCTCTGCTGATGACATAC
	Reverse primer	5′-GGTAGTGACAGCATCAAAACTCAAA –3′
	Probe	5′-FAM-TCCCTGTATGGAGACCCAAAAGAGAACCA-TAMRA –3′
MMP-13	Forward primer	5′-AAATTATGGAGGAGATGCCCATT –3′
	Reverse primer	5′-TCCTTGGAGTGGTCAAGACCTAA –3′
	Probe	5′-FAM-CTACAACTTGTTTCTTGTTGCTGCGCATGA-TAMRA –3′
MMP-14	Forward primer	5′-AAGGCCAATGTTCGAAGGAA –3′
	Reverse primer	5′-GGCCTCGTATGTGGCATACTC –3′
	Probe	5′-FAM-CAACATAATGAAATCACTTTCTGCATCCAGAATTACA-TAMRA –3′
MMP-15	Forward primer	5′-GCGCTTCAACGAGGAGACA –3′
	Reverse primer	5′-TCCAGTATTTGGTGCCCTTGT –3′
	Probe	FAM-CCTTCCTGAGCAATGACGCAGCCTAC-TAMRA –3′
MMP-16	Forward primer	5′-ATGATTTACAGGGCATCCAGAAA -'3
	Reverse primer	5′-TGAGGCCGAGGAGGTTT –3′
	Probe	5′-FAMCAAGATTCCTCCACCTACAAGACCTCTACCGAC-TAMRA –3′
MMP-17	Forward primer	5′-FAM-GCGGGTATCCTTCCTCTACGT –3′
	Reverse primer	5′-CAGCGACCACAAGATCGTCTT –3′
	Probe	5′-FAM-ATTGTCCTTGAACACCCAGTACCTGTCTCCTTAA-TAMRA –3′
MMP-19	Forward primer	5′-GGCTACCGGCCCCACTT –3′
	Reverse primer	5′-TGTCTCTTCTTCTTCCTCATCCCTTA –3′
	Probe	5′-FAM-ATCCAGGCTCTCTATGGCAAGAAGAGTCCA-TAMRA –3′
MMP-20	Forward primer	5′-CCTTTGACGCTGTGACAATGC –3′
	Reverse primer	5′-TCCTGTCCGCAAGTGAACCT –3′
	Probe	5′-FAM-TCCTGCTCTTCAAGGACCGGATTTTCTG-TAMRA –3′
MMP-21	Forward primer	5′-CCAGTGACACGGGCATCA –3′
	Reverse primer	5′-ATTATGGATCCCGTCCTGTAGGT –3′
	Probe	5′-FAM-CCTTCTCAAGGTGGCCGTCCATGA-TAMRA –3′

(*Continued on the following page*)

Table 2. Primers and probes used for quantitative Real-time RT-PCR (Cont'd)

MMP-23	Forward primer	5′-TCCACAAGAAAGGGAAAGTGTACTG –3′
	Reverse primer	5′-ACGGCGTTGGCGATGAT –3′
	Probe	5′-FAM-TTCTCCTACCCCGGCTACCTGGCC –3′
MMP-24	Forward primer	5′-CCAHTACATGGAGACGCACAA –3′
	Reverse primer	5′-TGCGGACGGGGAGTGT –3′
	Probe	5′-FAM-CAGGGCATCCAGAAGATCTATGGACCC-TAMRA –3′
MMP-25	Forward primer	5′-GACGATGAGGAGACCTGGACTTT –3′
	Reverse primer	5′-CCTGGTAGAAGGGCCTCATAATG –3′
	Probe	5′-FAM-CCGACCTGTTTGCCGTGGCTGTC –3′
MMP-26	Forward primer	5′-ACTTGTGGAAATCCTGGAGTTGTC –3′
	Reverse primer	5′-CAAAGAATGCCCAATCTCATGA –3′
	Probe	5′-FAM-CTGGTCAGCTTCAGACACTGGATATAATCTGTTCC-TAMRA –3′
MMP-27	Forward primer	5′-GTTTAGAAGTGTGGAGCAAAGTCACT –3′
	Reverse primer	5′-ATAGCGAGGACACCGACCAT –3′
	Probe	5′-FAM-CATCATGATTGCCTTTAGGACTCGAGTCCA-TAMRA–3′
MMP-28	Forward primer	5′-TTTGAGACCTGGGACTCCTACAG –3′
	Reverse primer	5′-CCCACGAAATGGCTCCCTTTA –3′
	Probe	5′-FAM-ACTCTTCCTTCGATGCCATCACTGTAGACAG-TAMRA –3′
ADAM-8	Forward primer	5′-AAGCAGCCGTGCGTCATC –3′
	Reverse primer	5′-AACCTGTCCTGACTATTCCAAATCTC –3′
	Probe	5′-FAM-AATCACGTGGACAAGCTATATCAGAAACTCAACTTCC-TAMRA –3′
ADAM-9	Forward primer	5′-GGAAACTGCCTTCTTAATATTCCAAA –3′
	Reverse primer	5′-CCCAGCGTCCACCAACTTAT –3′
	Probe	5′-FAM- CCTGATGAAGCCTATAGTGCTCCCTCCTGT-TAMRA –3′
ADAM-12	Forward primer	5′-CCTCAGACCTGCTCCACAATATC –3′
	Reverse primer	5′-TTGAAAAAAGGTGTCGGCTTCT –3′
	Probe	5′-FAM-ACCAAGTGCCCAGATCCACCCACAC-TAMRA –3′
ADAM-17	Forward primer	5′-GAAGTGCCAGGAGGCGATTA –3′
	Reverse primer	5′-CGGGCACTCACTGCTATTACC –3′
	Probe	5′-TGCTACTTGCAAAGGCGTGTCCTACTGC-TAMRA –3′
ADAM-28	Forward primer	5′-GGGCCCACGATTTGCA –3′
	Reverse primer	5′-TGAACCTTCCTGTCTTTCAATTTTACT –3′
	Probe	5′-FAM-AGAACATTGCCCTACCTGCCACCAAAC-TAMRA –3′

used to track protein migration. The proteins were transferred to Immobilon-P^{SQ} membrane (Millipore) at 45 V overnight in TG transfer buffer (Bio-Rad Laboratories Ltd) containing 20% (v/v) methanol (Fisher-Scientific). The membrane was then washed in wash buffer containing 20 mmol/L Tris-HCl (pH 7.6), 1.3 mol/L NaCl, and 0.1% (v/v) Tween 20 (Sigma-Aldrich) before blocking for 1 h in wash buffer containing 5% Marvel (Premier International Foods Ltd). After further washes in wash buffer, the membrane was incubated with the primary antibody [sheep anti-human MMP3 at 20 μg/mL, MMP14 at 5 μg/mL (31) according to the manufacturers instructions] in blocking buffer overnight at 4°C. The membrane was then washed before applying the secondary antibody [peroxidase anti-sheep (Stratech Scientific Ltd) or peroxidase anti-rabbit (Vector Laboratories)] according to manufacturers instructions, for 1 h at room temperature. Finally the membrane was washed and visualized using the ECL Plus detection kit (GE Healthcare UK Ltd). After use, the membranes were stained for total protein in Coomassie stain for 30 min and then destained in 10% (v/v) acetic acid and 30% (v/v) isopropanol.

Expression of ADAM8, ADAM9, and ADAM28 in NHEKs and HNSCC cells was analyzed by Western blotting. Cell lysates from HNSCC and normal keratinocyte cultures were collected and aliquots were fractionated on SDS-polyacrylamide gels, transferred to Hybond enhanced chemiluminescence nitrocellulose membrane (Amersham Pharmacia Biotech. The membranes were blocked using 5% skimmed milk. Proteins were detected using goat anti-human ADAM8 antibodies (AF1031) or goat anti-human ADAM9 polyclonal antibodies (AF939; both from R&D Systems), mouse monoclonal ADAM28 antibody (297-2F3; ref. 32), and peroxidase-conjugated secondary antibodies. The blots were visualized by enhanced chemiluminescence detection system (Amersham Pharmacia Biotech).

Statistical analyses. Statistical analysis to compare expression between the tissue types and the clinicopathologic variables was done using the Kruskall-Wallis ANOVA

with Dunn's multiple comparison tests for those found to show significance by ANOVA or Mann-Whitney nonparametric unpaired *t* testing. Statistical comparison between HNSCC cell lines and NHEKs was performed using Wilcoxon rank-sum test.

Results

Global analysis of the expression of degradome components in distinct compartments of HNSCC tumor tissue. To obtain a comprehensive view of the expression of degradome components in distinct compartments of HNSCCs, quantitative real-time reverse transcription-PCR (RT-PCR) was used for the expression profiling of the entire MMP and TIMP families, as well as selected ADAMs and ADAMTSs in a large panel consisting of 83 samples from the non-necrotic center of the head and neck tumors, 41 samples from the invasive margin of the tumors, and 41 samples from the tissue adjacent to the tumors. These tumor samples were compared with 13 normal non-neoplastic uvular mucosal samples from individuals without carcinomas. The expression data for all MMPs, TIMPs, ADAMs, and ADAMTSs profiled are summarized in Fig. 1A, which shows a heat map representation of the average cycle threshold (CT) values for each gene to allow the comparison

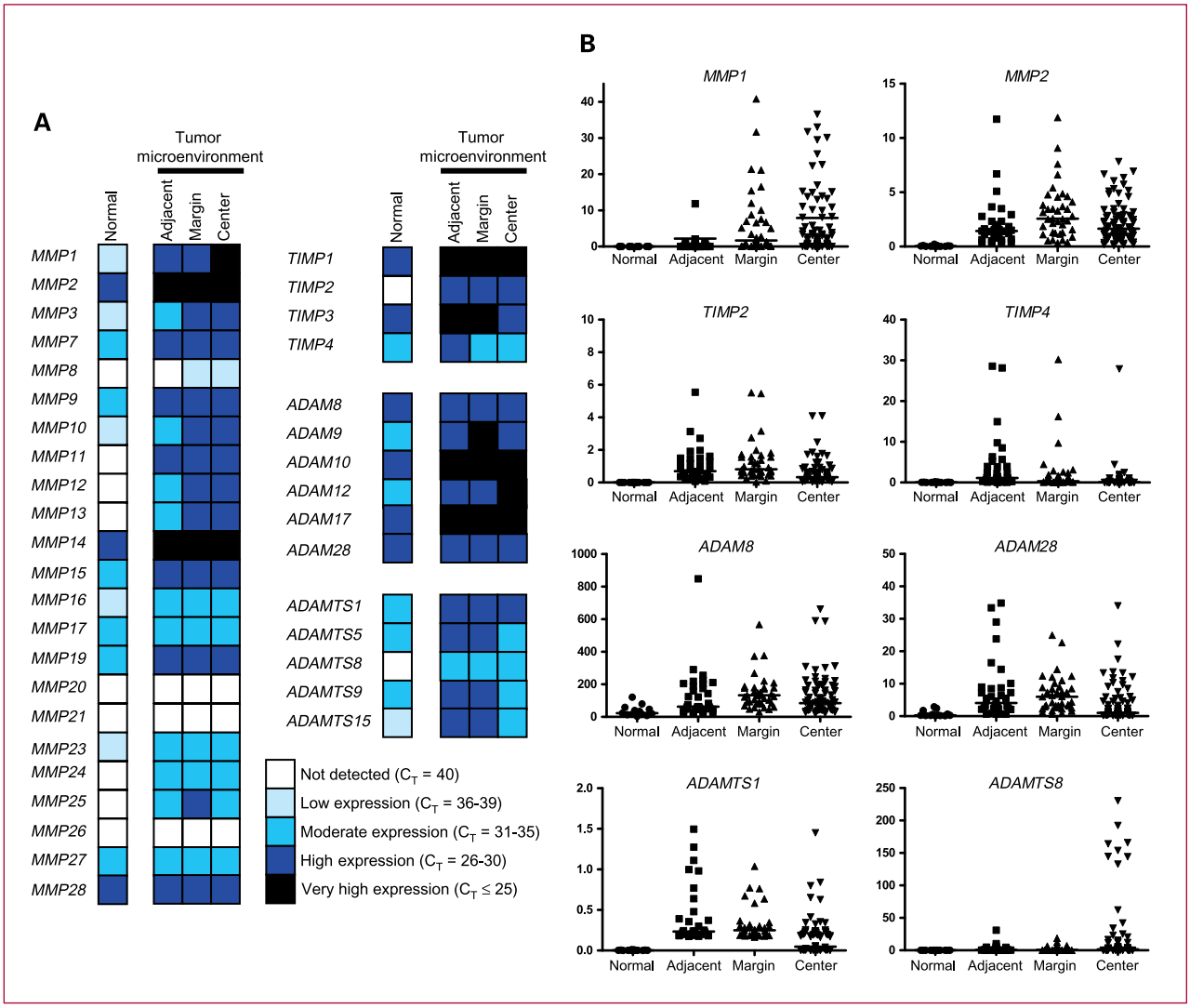

Fig. 1. Expression of degradome components in distinct compartments of head and neck SCC tumor tissue. A, the expression of degradome components in distinct RNA extracted from distinct tissue compartments of HNSCC tumors (n = 83) and normal mucosal tissue (n = 13) was determined by quantitative real-time RT-PCR. Colored tiles, the mean CT values; white tiles, median CT values of 40; light blue tiles, median CT values of 36 of 39; medium blue tiles, median CT values of 31 to 35; dark blue tiles, median CT values of 26 to 30; and black tiles, median CT values of ≤25. B, the expression of selected degradome components in distinct HNSCC tissue compartments and normal tissue was determined by quantitative real-time RT-PCR. The median values are shown by horizontal bars. Statistical analysis was done using Kruskall-Wallis ANOVA with Dunn's multiple comparison tests for those found to show significance by ANOVA. The *P* values for this analysis are detailed in Table 3.

of approximate overall levels of expression between different genes (29). In addition, scatter plots for selected genes are shown in Fig. 1B, allowing the precise quantification of changes in expression for single genes between different specimens and comprehensive comparison between distinct tumor compartments is shown in Table 3. The data show that

Table 3. Comparison of the differences in degradome component expression between distinct head and neck SCC tumor tissue compartments and normal tissue

Gene	Normal epithelium compared with tumor compartments			Comparison within tumor compartments		
	Normal vs Adjacent	Normal vs Margin	Normal vs Center	Adjacent vs Margin	Adjacent vs Center	Margin vs Center
MMP1	**	***	***	***	***	Ns
MMP2	***	***	***	Ns	Ns	Ns
MMP3	**	***	***	*	Ns	Ns
MMP7	*	***	***	Ns	*	Ns
MMP8	Ns	Ns	*	Ns	***	Ns
MMP9	**	***	***	Ns	**	Ns
MMP10	**	***	***	Ns	***	Ns
MMP11	**	***	***	Ns	***	Ns
MMP12	***	***	***	**	***	Ns
MMP13	*	***	***	Ns	***	Ns
MMP14	**	***	***	*	***	Ns
MMP15	Ns	Ns	Ns	Ns	**	**
MMP16	***	***	***	Ns	Ns	Ns
MMP17	***	***	***	Ns	Ns	Ns
MMP19	**	***	***	Ns	Ns	Ns
MMP23	***	***	***	Ns	Ns	*
MMP24	***	***	***	Ns	***	***
MMP25	***	***	***	Ns	Ns	**
MMP27	Ns	Ns	Ns	Ns	***	***
MMP28	*	*	Ns	Ns	Ns	Ns
TIMP1	***	***	***	Ns	Ns	**
TIMP2	***	***	***	Ns	*	***
TIMP3	***	***	**	Ns	**	**
TIMP4	***	***	Ns	Ns	***	***
ADAM8	**	***	***	Ns	Ns	Ns
ADAM9	***	***	***	Ns	Ns	**
ADAM10	***	***	***	Ns	*	***
ADAM12	***	***	***	Ns	Ns	*
ADAM17	***	***	***	Ns	Ns	**
ADAM28	***	***	*	Ns	**	***
TS1	***	***	***	Ns	***	***
TS5	***	***	**	Ns	***	***
TS8	***	***	***	Ns	Ns	Ns
TS9	***	***	Ns	Ns	***	***
TS15	***	***	***	Ns	Ns	*

NOTE: The expression of degradome components in distinct HNSCC tissue compartments (center, margin, adjacent) and normal tissue was determined by quantitative real-time RT-PCR. Black shading, an increase in expression, e.g., for *MMP1,* expression is significantly increased in all tissue samples compared with normal samples. Gray shading, a decrease in expression, e.g., for *MMP2,* expression is decreased in the center samples compared with margin samples. The statistical analysis was done by Kruskall-Wallis ANOVA with Dunn's multiple comparison tests for those proteases found to show significance by ANOVA. The *P* values of 0.01 to 0.05 (*), 0.001 to 0.01 (**), and <0.001 (***) are shown.

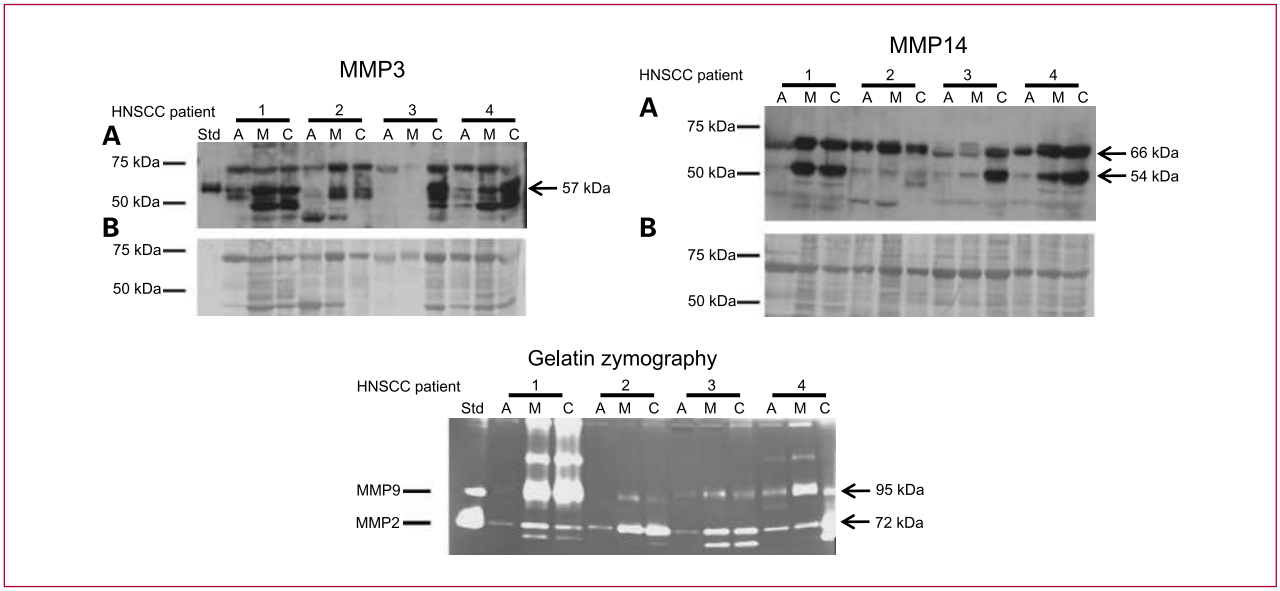

Fig. 2. Expression MMP 3, 14, 2, and 9 in distinct compartments of head and neck SCC tumors. Protein was extracted from matched normal (N), margin (M), and center (C) tissues of six HNSCC patients (1-6). Western blotting was done on four of these protein sets for MMP3 and MMP14 (A, top. Arrows, proMMP3 (57 kDa; left top) and proMMP14 (66 kDa) and active MMP14 (54 kDa; right top). After Western blotting, the membrane was stained for total protein using Coomassie blue stain (B, bottom). Gelatin zymography was done using protein extracted from matched normal, margin, and center tissues of six HNSCC patients (1-6). A positive control was loaded onto the zymography identifying an ~95-kDa band of latent MMP-9 and an ~72-kDa band of latent MMP-2.

the expression of the majority of MMPs in normal tissue is low or undetectable with the exception of *MMP2*, *MMP14*, and *MMP28*. The expression of *MMP8*, *MMP11*, *MMP12*, *MMP13*, *MMP24*, and *MMP25* was not detected in normal mucosa but was abundant in tumor tissue (Fig. 1A). The majority of the MMPs were expressed in tumor tissues, both in the center and the invasive margin of the tumor and the expression was in general increased compared with normal tissue (Table 3; Fig. 1A). Expression of most MMPs was also noted in the adjacent tissue, and for some MMPs, the level was lower than in tumor tissue. The only MMP with significantly decreased expression in the center tissues compared with adjacent tissues was *MMP27* (Table 3).

Abundant expression of members of the ADAM family was noted in the tumor tissue and adjacent tissue, and the expression levels were also largely increased in tumor tissues, with no ADAM showing significantly decreased expression (Fig. 1A). Members of the ADAMTS family examined showed low expression in normal tissue with no detectable expression of *ADAMTS8*. High or moderate expression of all ADAMTSs was noted in the tumor tissue (Fig. 1A). *ADAM8* and *ADAM28* were expressed in all compartments of the tumor and there was no marked difference between expression in tumor tissue and adjacent tissue (Table 3; Fig. 1B). In comparison, *ADAMTS8* expression was higher in the tumor center with low expression in the tumor margin, which was opposite to the pattern for *ADAMTS5*, *9*, and *15*, which were expressed at a lower level in the center tumor samples (Table 3; Fig. 1A). Of the proteinase inhibitors, markedly increased expression of *TIMP2* was noted in tumor tissues, whereas the expression in normal tissue samples was undetectable (Fig. 1A and B). *TIMP4* expression was very low in normal oral tissue, highest in tissue adjacent to tumor, and decreasing in the tumor margins and center (Table 3; Fig. 1A and B). No expression of *MMP20*, *21*, and *26* was found in any of these tissues, with median CT values of 40 (Fig. 1A).

Proteinase protein levels in HNSCC tissues. Western blot analysis and gelatin zymography were done to assess the levels of selected proteinases, i.e., MMP2, MMP3, MMP9, and MMP14 in the adjacent, margin, and center tissues. The protein levels of these proteinases largely followed the mRNA levels increasing in the tumor margin and center compared with the adjacent tissues (Fig. 2). Coomassie blue total protein staining confirmed even protein loading for tissue samples used in Western blotting. Consistent with the mRNA and protein increases seen for MMP14, the major enzyme responsible for the activation of pro-MMP2 in the tumor margin and center samples, increased levels of active MMP2 were noted in these samples by zymography.

Degradome component expression by HNSCC tumor cell lines. To verify the specific expression of MMPs, ADAMs, and ADAMTSs by tumor cells of HNSCCs, we performed expression profiling of a large panel of cell lines (n = 34) established from these tumors. Based on the analysis of the *in vivo* tissue samples, the quantitative real-time RT-PCR expression data for selected MMPs, TIMPs, ADAMs, and ADAMTSs profiled are summarized in Fig. 3A. The data show that most of the MMPs are expressed at high level in

HNSCC tumor cell lines compared with normal keratinocytes with only few exceptions. The highest increases in the levels in SCC cells were noted in *MMP2*, *MMP7*, *MMP10*, *MMP11*, *MMP13*, *MMP14*, *MMP16*, *MMP17*, *MMP23*, *MMP24*, and *MMP25* (Fig. 3A). The only MMP showing decreased expression in SCC cells was *MMP27*

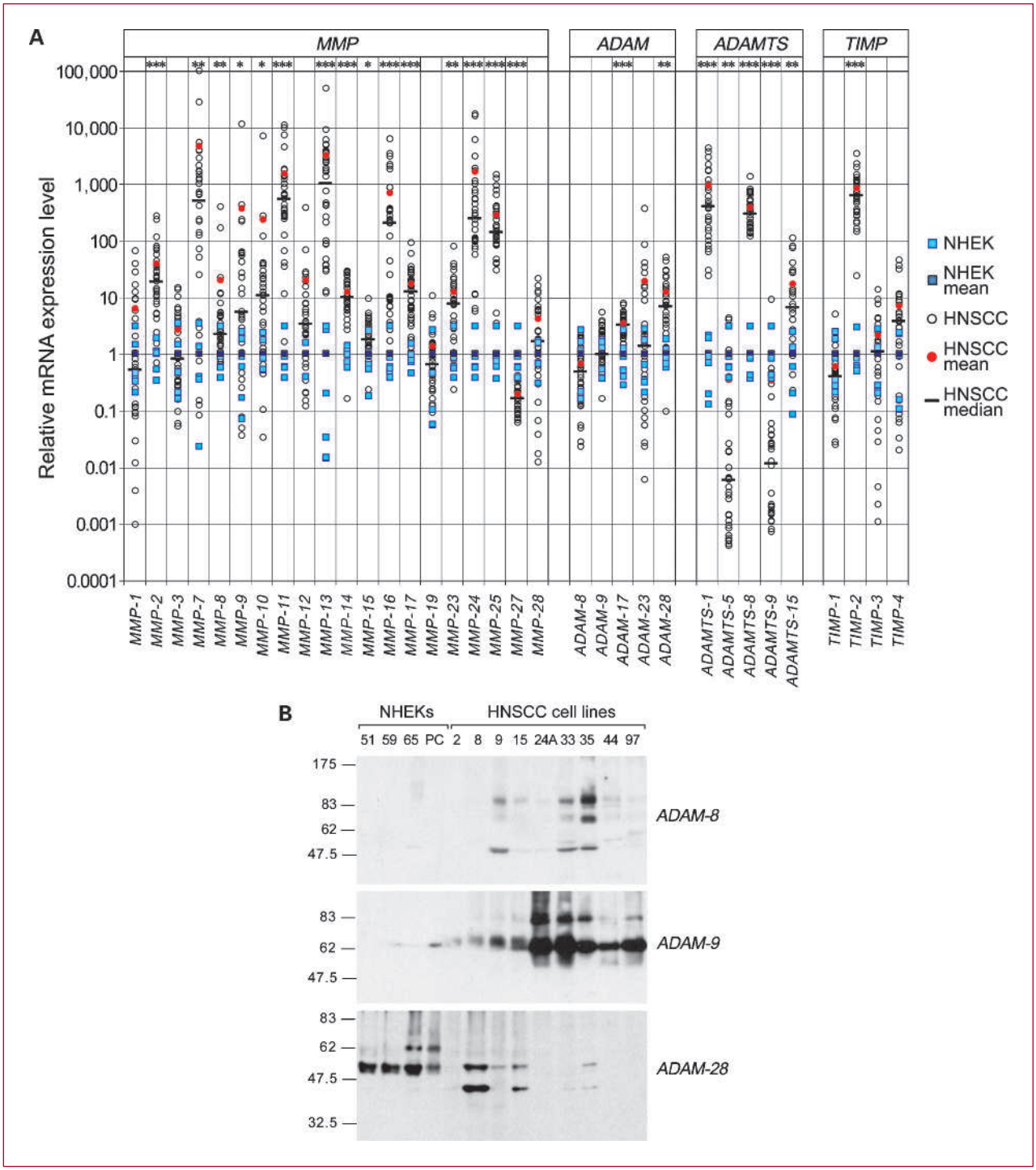

Fig. 3. Expression of degradome components by head and neck SCC tumor cell lines. A, expression of degradome components in HNSCC cell lines (n = 34) was determined by quantitative real-time RT-PCR, normalized to 18S rRNA levels in each sample, and compared with the levels in NHEKs (1.00). Statistical comparison between HNSCC cell lines and NHEKs was performed using Wilcoxon rank-sum test and P values for 0.01 to 0.05 (*), 0.001 to 0.01 (**), and <0.001 (***) are shown. B, expression of ADAM8, ADAM9, and ADAM28 by NHEKs and selected HNSCC cell lines (n = 9) were determined by Western blotting of cell lysates. Left, positions of molecular weight markers (in kDa).

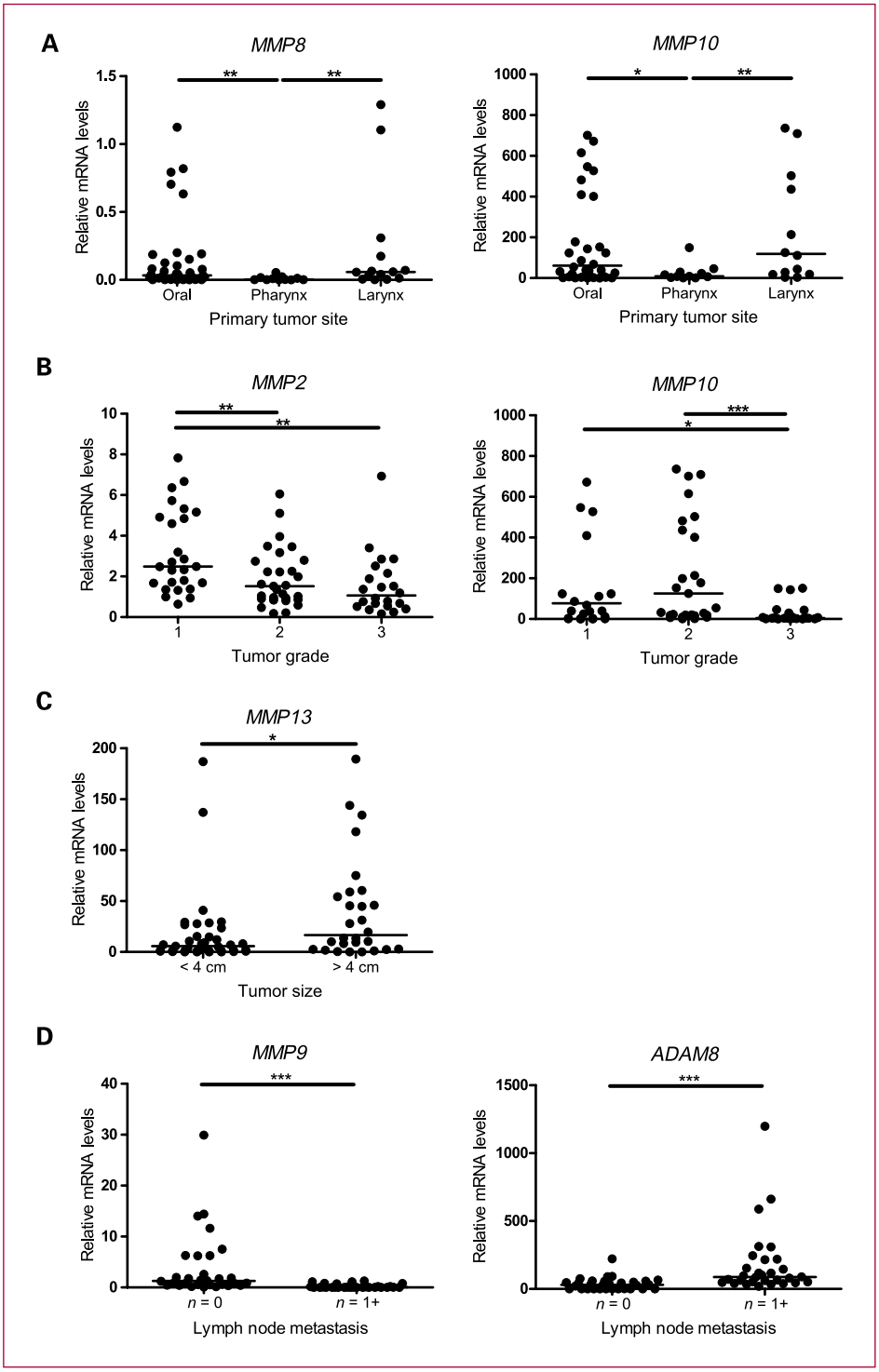

Fig. 4. Correlation of the expression of selected proteinases with clinical parameters. HNSCC patients were separated into groups according to (A) location of the primary tumor (oral cavity, pharynx, and larynx; B) histopathologic grade of the primary tumor (grade 1, well differentiated; grade 2, moderately differentiated; grade 3, poorly differentiated), (C) local invasion of primary tumor (size > 4 cm), and (D) lymph node metastasis (N1+). The real-time PCR data normalized to 18S were analyzed between these groups using Mann-Whitney nonparametric unpaired *t* testing. Selected proteinases that displayed significant changes between these groups are shown. The median values are shown as horizontal bars within the data and significant differences are represented as *, **, or *** for *P* values of 0.01 to 0.05, 0.001 to 0.01, or <0.001, respectively. Where there are more than two groups for statistical testing, horizontal bars identify the two parameters between which significant differences were found.

($P < 0.05$). Among the ADAMs analyzed, *ADAM17* and *ADAM28* were expressed at higher levels in SCC cells. *ADAMTS8* was the only analyzed degradome component found absent in all normal epidermal keratinocyte samples, with median CT values of 40. *ADAMTS1* and *ADAMTS15* were clearly upregulated in SCC cells compared with normal keratinocytes. In contrast, the expression of *ADAMTS5* and *ADAMTS9* was clearly decreased in SCC cells. Expression of TIMPs was observed both in SCC cells and normal keratinocytes with *TIMP4*, and especially *TIMP2*, showing significantly increased expression in tumor cells. In summary, the alterations in proteinase

expression levels in HNSCC cell lines were in good agreement with the results obtained with tumor material (Figs. 1A and B, and 3A).

Expression of ADAMs by HNSCC tumor cells. The expression of novel HNSCC proteinases, ADAM8, ADAM9, and ADAM28, was further analyzed by Western blotting of lysates of cultured HNSCC cells. A 100-kDa band was noted in the ADAM8 Western blot in HNSCC tumor cells (Fig. 3B). ADAM8 is produced as a 92-kDa proform, but due to posttranslational modifications, its molecular mass on the cell surface is ~100 kDa (33), corresponding in size to the largest band seen in the HNSCC samples (Fig. 3B). A 72-kDa band was also observed, apparently representing a form of ADAM8 generated by proteolytic removal of the prodomain. The smallest species, ~50 kDa in size, may represent ADAM8 lacking the metalloproteinase domain. A marked variation in the expression levels of ADAM8 protein between distinct HNSCC cell lines analyzed was noted (Fig. 3B), and the levels in individual cell lines correlated well with the corresponding mRNA levels (data not shown). Production of an ~84-kDa mature ADAM9 was detected in all HNSCC cell lines examined, and the expression levels were also variable between individual cell lines (Fig. 3B) and correlated with the corresponding mRNA levels (data not shown). The 60- to 65-kDa band detected may represent an ADAM9-like protein, which is also detected with the ADAM9 antibody used (34). In the same HNSCC cells, ADAM28 bands of 55 and 42 kDa in size were detected in most HNSCC cell lines (Fig. 3B). The 55-kDa band is considered to be propeptide-deleted membrane-bound ADAM28 and the 42-kDa form of ADAM28 is an active form (32). In summary, these results show that ADAM8, ADAM9, and ADAM28 are readily expressed by tumor cells of HNSCCs.

Degradome component expression and HNSCC clinicopathologic parameters. Clinical information about primary tumor location, size, histopathologic grade, and presence of lymph node metastases was available for all 83 HNSCC patients. The quantitative real-time RT-PCR expression data were further analyzed for differences in degradome gene expression with respect to these clinical parameters. In general, there were few significant differences in degradome gene expression between primary tumors differing in location, grade, and size. However, certain differences were noted in tumors based on anatomic location. *MMP8* and *10* were mainly expressed by tumors of oral cavity and larynx and *MMP17* in tumors of oral cavity (Fig. 4A and not shown). Increased expression of *MMP1* and *3* was seen in tumors of the oral cavity compared with the pharynx (data not shown). In contrast, *ADAM8*, *9*, and *28* were expressed preferably in SCCs of pharynx (data not shown).

Certain significant differences in expression were also noted between tumors representing different histopathologic grades, i.e., different levels of differentiation. Specifically, there was a significant decrease in the expression of *MMP2* with tumor grade, the highest expression being noted in well differentiated (grade 1) tumors (Fig. 4B). Similarly, a decrease in *MMP10* expression was noted in poorly (grade 3) differentiated tumors. Interestingly, the expression of *ADAM8*, *9*, and *17* was significantly higher in grade 2 and 3 tumors and the expression of *ADAM28* was highest in grade 2 tumors (data not shown).

With respect to tumor size, a significant increase was noted in *MMP13* expression in locally invasive tumors with size over 4 cm (Fig. 4C). No other significant differences about tumor size were found. Significant differences were also detected in the expression of degradome components in primary tumors of patients with lymph node metastases (Fig. 4D). *MMP9* showed significant decrease in expression in tumors with regional metastasis, whereas an increase in the expression of *ADAM8* was noted in the same metastatic tumors (Fig. 4D).

Discussion

The data presented in this study represent the first time that the expression of so many proteinases and their inhibitors has been studied as molecular markers in tumors of HNSCC patients. Utilization of a highly sensitive and specific quantitative technique (real-time PCR) to measure their expression in normal tissues from patients without carcinomas, peritumoral tissues adjacent to head and neck tumors, and two distinct tumor tissues (margin and nonnecrotic center tumor samples) of a fairly large patient cohort means that the role of these enzymes and their inhibitors in HNSCC can now be evaluated. The altered expression of proteinases and their inhibitors specifically in tumor cells were further investigated with cell lines derived from HNSCC tumors and with normal keratinocytes.

The patient cohort used in this study included 83 HNSCC patients of all ages, tumor stages, metastatic status, and primary tumor sites. Cell lines were established from 34 tumors of these patients. Together, the data presented correspond to a diverse and heterogeneous group of patients. However, to provide a descriptive degradome of HNSCC, the profiling data were presented in Fig. 1A and B and Table 3 as a whole with no selection of the patients from this group. It is recognized that this may dilute significant trends that could be attributed to individual patient and tumor characteristics. However, we have addressed this issue and some interesting differences between different clinicopathologic groups were apparent, as shown in Fig. 4. However, it is likely that this patient cohort is still too small for many significant trends to be detected. In addition, the analyses of both normal tissue samples and tumor adjacent tissue samples also clearly show that the peritumoral adjacent tissue is strongly affected by the tumor and therefore cannot be considered as a normal tissue (Table 3; Fig. 1A and B). We summarized below our key observations in relation to previous studies of particular proteinases and inhibitors in HNSCC.

MMPs and TIMPs. The descriptive degradome data of the MMPs for the most part confirm existing data on their expression in HNSCC. O-Charoenrat et al. (35) used semiquantitative RT-PCR analysis of tissue homogenates from

54 HNSCC patients to study many of the MMPs. In accordance with their data, we show that *MMP1*, *2*, *3*, *7*, *9*, *10*, *11*, *13*, and *TIMP1* were increased in tumor tissues compared with normal tissues (Table 3; Fig. 1). It was also possible to confirm some of these findings at the protein level (Fig. 2). Furthermore, the analysis of HNSCC tumor cell lines showed clearly increased levels of *MMP2*, *7*, *9*, *10*, *11*, *13*, *14*, *16*, *17*, *23*, *24*, and *25*, indicating that these proteinases are produced by malignant cells of these tumors. These findings are in accordance with previous studies using immunohistochemistry and *in situ* hybridization, as well with recent studies with quantitative RT-PCR (28, 36).

Interestingly, in divergence from the study of O-Charoenrat et al. (35), we also show that the expression of *MMP14* and *TIMP2* was increased in tumor tissues compared with normal tissues in this study (Table 3; Fig. 1A and B). Increased expression of *MMP14* was also seen with SCC cell lines, indicating that this altered expression is indeed due to the malignant transformation of these cells (Fig. 3A). Increased MMP14 in HNSCC tumors has been reported previously (37). In addition, MMP14 is overexpressed by carcinoma-associated fibroblasts from HNSCC patients and *MMP14* and *MMP2* overexpression together has been shown to increase their invasion *in vitro* (38). TIMP2 protein levels, while not previously reported to be increased in tumor tissues compared with normal tissues, correlate with lymph node metastasis and poor prognosis of early-stage oral HNSCC (39), suggesting that TIMP2 also has a role in progression of HNSCC tumors. Cell-mediated activation of pro-MMP2 involves its binding to a complex formed by MMP14 and TIMP2. This anchorage of the pro-MMP2 molecule to the cell surface allows a second MMP14, which is not bound by TIMP2, to cleave and activate the pro-MMP2. Therefore, with high activation of MMP2 shown by the gelatin zymography (Fig. 2), it is possible that the increased expression of both MMP14 and TIMP2 in these tumors could reflect their roles in the activation of MMP2, further enhancing the effect of upregulated MMP2 levels seen in both *in vivo* (Table 3; Fig. 1A and B) and *in vitro* (Fig. 3A).

The remaining MMPs also showed significant increases in expression in the tumor tissues compared with adjacent peritumoral tissues. The only exception was *MMP27* (Table 3), which was the only MMP to significantly decrease in expression in tumor center and malignant cell lines, suggesting a potentially protective role of this proteinase in HNSCC progression. Certain differences were also detected in the expression of MMPs in locally invasive and metastatic primary tumors. Increased expression of *MMP13* expression was noted in large locally invasive tumors (Fig. 4C). In contrast, *MMP9* expression was significantly decreased in tumors with lymph node metastasis (Fig. 4D). *TIMP4* was also the only TIMP significantly decreased in its expression in tumor tissues compared with adjacent tissue. Interestingly, these decreases in *MMP27* and *TIMP4* expression at the mRNA level have also been seen in other tumor types including prostate cancer (25), glioma (40), and breast cancers.[11] Although *MMP27* cannot be detected by real-time PCR, *TIMP4* is significantly decreased in expression in prostate cancers (25). These findings suggest that both MMP27 and TIMP4, which have been little studied in the cancer field to date, are worthy of further functional investigation in relation to their roles in the pathophysiology of HNSCC. With further overlap in proteinase expressions between these three tumor types in those proteinases increased in HNSCC tumor tissues, this indicates that some proteinases and proteinase inhibitors might be particularly important in tumorigenesis of all types epithelial cancers.

ADAMs and ADAMTSs. Like the MMPs, the profiled ADAMs, which mediate growth factor shedding and regulate adhesion and motility, were significantly increased in their expression in the HNSCC tumor tissues compared with normal tissues (Table 2; Fig. 1A and B). Previous studies have shown that several members of the ADAM family are upregulated in at least one cancer type (reviewed in ref. 13), but there are only a few studies about HNSCCs. There is some suggestion to their involvement in HNSCC as both ADAM10 (21) and ADAM12 (22) are overexpressed in oral HNSCCs. However, this is the first time that *ADAM8*, *9*, *17*, and *28* have been associated with HNSCC. Although detailed localization data are not yet available, the expression levels in the tumor-derived cell lines strongly suggest that at least *ADAM17* and *28* are expressed by the malignant cells in tumors (Fig. 3A). These results were also confirmed at the protein level ADAM8, 9, and 28 in SCC cell lines (Fig. 3B). In addition, increased expression of *ADAM8* was noted in the metastatic tumors (Fig. 4D). Together these data strongly suggest that certain ADAMs, most convincingly ADAM8, ADAM17, and ADAM28, have an important role in HNSCC pathogenesis. Detection of the 42-kDa band in the ADAM28 Western blot also showed that ADAM28 is proteolytically activated in a subset of HNSCC cell lines (Fig. 3B). ADAM28 has shown to be overexpressed in breast carcinoma cells and to increase their proliferation (41). Accordingly, our data suggest that ADAM28 could also function in tumorigenesis of HNSCCs.

Studies about ADAMTSs in human cancers have revealed different and often contradictory roles of certain ADAMTSs between different types of cancer (42). In particular, ADAMTS1 and 8 are antiangiogenic and thus potentially antagonistic to tumor growth (43). However, ADAMTS1 has been shown to both promote or inhibit breast tumor growth and metastasis *in vivo*, depending on whether it is present as a full-length or cleaved molecule (44). Despite this, there is growing recognition that several ADAMTS family members are tumor suppressors (9). This is the case for *ADAMTS15* whose elevated expression correlates with favorable outcome in patients with breast cancer (45) and which acts as a functional tumor suppressor in colorectal cancer (46). Recently, of great relevance, *ADAMTS9* is deleted or silenced by methylation in esophageal SCC (47). We found only one previous study that has profiled ADAMTSs in the context of HNSCC (48).

[11] Pennington, C.J., and Edwards, D.R., unpublished observations.

The results of their study showed that the mRNA levels of *ADAMTS1*, *4*, *5*, *8*, *9*, and *15* were all reduced in HNSCC primary tumors compared with paired noncancerous tissues in a cohort of 20 patients. Interestingly, these authors found all but *ADAMTS4* increased in metastatic tissue compared with primary tumor tissue. The results of our study agree with these findings when comparing tumor center and peritumoral adjacent tissue, with the exception of *ADAMTS8* (Table 3; Fig. 1A and B). However, when comparing tumor center samples to normal tissue samples, *ADAMTS1*, *5*, *8*, and *15* were increased in expression, whereas *ADAMTS9* was the only analyzed ADAMTS, the expression of which did not significantly differ between the center tumor tissues and normal tissues (Table 3; Fig. 1A and B). Tumor cell lines established from HNSCCs showed clearly decreased expression of *ADAMTS5* and *9*, and strongly increased expression of *ADAMTS1*, *8*, and *15* compared with normal keratinocytes (Fig. 3A). These results show that there is major dysregulation of multiple members of the ADAMTS family, i.e., *ADAMTS1*, *8*, and *15* in HNSCCs, suggesting a role for these proteinases in HNSCC progression.

In conclusion, the current study provides the most comprehensive analysis to date of the expression of metalloproteinases and their inhibitors in HNSCC. In addition to endorsing roles for several previously studied MMPs and TIMPs, these data highlight several additional novel metalloproteinase genes showing altered expression in tumor tissues and cell lines, including *ADAM8*, *ADAM17*, *ADAM28*, *ADAMTS1*, *ADAMTS8*, *ADAMTS9*, and *ADAMTS15*. Based on emerging knowledge from other tumor types, further studies into the clinical significance of these novel HNSCC-associated proteinases are likely to prove fruitful.

Disclosure of Potential Conflicts of Interest

No potential conflicts of interest were disclosed.

Acknowledgments

We thank Merja Lakkisto, Sari Pitkänen and Johanna Markola for their skillful assistance.

Grant Support

The Academy of Finland (project 114409), the Finnish Cancer Research Foundation, Sigrid Juselius Foundation, Turku University Central Hospital EVO grant (project 13336), European Union Framework Programme 6 (LSHC-CT-2003-503297) and by Turku University Foundation (J. Joutsa) The Big C Appeal, The Anthony Long Charitable Trust.

The costs of publication of this article were defrayed in part by the payment of page charges. This article must therefore be hereby marked *advertisement* in accordance with 18 U.S.C. Section 1734 solely to indicate this fact.

Received 09/16/2009; revised 12/18/2009; accepted 01/01/2010; published OnlineFirst 03/21/2010.

References

1. Parkin DM, Bray F, Ferlay J, Pisani P. Global cancer statistics, 2002. CA Cancer J Clin 2005;55:74–108.
2. Brennan JA, Mao L, Hruban RH, et al. Molecular assessment of histopathological staging in squamous-cell carcinoma of the head and neck. N Engl J Med 1995;332:429–35.
3. Sotiriou C, Lothaire P, Dequanter D, Cardoso F, Awada A. Molecular profiling of head and neck tumors. Curr Opin Oncol 2004;16:211–4.
4. Lopéz-Otín C, Overall CM. Protease degradomics: a new challenge for proteomics. Nat Rev Mol Cell Biol 2002;3:509–19.
5. Skrzydlewska E, Sulkowska M, Koda M, Sulkowski S. Proteolytic-antiproteolytic balance and its regulation in carcinogenesis. World J Gastroenterol 2005;11:1251–66.
6. Egeblad M, Werb Z. New functions for the matrix metalloproteinases in cancer progression. Nat Rev Cancer 2002;2:161–74.
7. Blobel CP. ADAMs: key components in EGFR signalling and development. Nat Rev Mol Cell Biol 2005;6:32–43.
8. Edwards DR, Handsley MM, Pennington CJ. The ADAM metalloproteinases. Mol Aspects Med 2008;29:258–89.
9. Lopez-Otín C, Matrisian LM. Emerging roles of proteases in tumour suppression. Nat Rev Cancer 2007;7:800–8.
10. Brinckerhoff CE, Matrisian LM. Matrix metalloproteinases: a tail of a frog that became a prince. Nat Rev Mol Cell Biol 2002;3:207–14.
11. Baker AH, Edwards DR, Murphy G. Metalloproteinase inhibitors: biological actions and therapeutic opportunities. J Cell Sci 2002;115:3719–27.
12. Hernandez-Barrantes S, Toth M, Bernardo MM, et al. Binding of active (57 kDa) membrane type 1-matrix metalloproteinase (MT1-MMP) to tissue inhibitor of metalloproteinase (TIMP)-2 regulates MT1-MMP processing and pro-MMP-2 activation. J Biol Chem 2000;275:12080–9.
13. Apte SS. A disintegrin-like and metalloprotease (reprolysin-type) with thrombospondin type 1 totif (ADAMTS) superfamily: functions and mechanisms. J Biol Chem 2009;284:31493–7.
14. Porter S, Clark IM, Kevorkian L, Edwards DR. The ADAMTS metalloproteinases. Biochem J 2005;386:15–27.
15. Amour A, Slocombe PM, Webster A, et al. TNF-a converting enzyme (TACE) is inhibited by TIMP-3. FEBS Lett 1998;435:39–44.
16. Amour A, Knight CG, Webster A, et al. The *in vitro* activity of ADAM-10 is inhibited by TIMP-1 and TIMP-3. FEBS Lett 2000;473:275–9.
17. Kashiwagi M, Tortorella M, Nagase H, Brew K. TIMP-3 is a potent inhibitor of aggrecanase 1 (ADAM-TS4) and aggrecanase 2 (ADAM-TS5). J Biol Chem 2001;276:12501–4.
18. Rosenthal EL, Matrisian LM. Matrix metalloproteases in head and neck cancer. Head Neck 2006;28:639–48.
19. Thomas GT, Lewis MP, Speight PM. Matrix metalloproteinases and oral cancer. Oral Oncol 1999;35:227–33.
20. Werner JA, Rathcke IO, Mandic R. The role of matrix metalloproteinases in squamous cell carcinomas of the head and neck. Clin Exp Metastasis 2002;19:275–82.
21. Ko SY, Lin SC, Wong YK, Liu CJ, Chang KW, Liu TY. Increase of disintergin metalloprotease 10 (ADAM10) expression in oral squamous cell carcinoma. Cancer Lett 2007;245:33–43.
22. Kornberg LJ, Villaret D, Popp M, et al. Gene expression profiling in squamous cell carcinoma of the oral cavity shows abnormalities in several signaling pathways. Laryngoscope 2005;115:690–8.
23. Pitchers M, Stokes A, Lonsdale R, Premachandra DJ, Edwards DR. Research tissue banking in otolaryngology: organization, methods and uses, with reference to practical, ethical and legal issues. J Laryngol Otol 2006;120:433–8.
24. Porter S, Scott SD, Sassoon EM, et al. Dysregulated expression of adamalysin-thrombospondin genes in human breast carcinoma. Clin Cancer Res 2004;10:2429–40.
25. Riddick AC, Shukla CJ, Pennington CJ, et al. Identification of degradome components associated with prostate cancer progression by expression analysis of human prostatic tissues. Br J Cancer 2005;92:2171–80.

26. Chomczynski P, Sacchi N. Single-step method of RNA isolation by acid guanidinium thiocyanate-phenol-chloroform extraction. Anal Biochem 1987;162:156–9.
27. Grénman R, Pekkola Heino K, Joensuu H, Aitasalo K, Klemi P, Lakkala T. UT-MUC-1, a new mucoepidermoid carcinoma cell line and its radiation sensitivity. Arch Otolaryngol Head Neck Surg 1992;118:542–7.
28. Junttila MR, Ala-Aho R, Jokilehto T, et al. p38α and p38δ mitogen-activated protein kinase isoforms regulate invasion and growth of head and neck squamous carcinoma cells. Oncogene 2007;26: 5267–79.
29. Nuttall RK, Pennington CJ, Taplin J, et al. Elevated membrane-type matrix metalloproteinases in gliomas revealed by profiling proteases and inhibitors in human cancer cells. Mol Cancer Res 2003;1:333–45.
30. Wall SJ, Edwards DR. Quantitative reverse transcription-polymerase chain reaction (RT-PCR): a comparison of primer-dropping, competitive, and real-time RT-PCRs. Anal Biochem 2002;300:269–73.
31. d'Ortho MP, Stanton H, Butler M, Atkinson SJ, Murphy G, Hembry RM. MT1-MMP on the cell surface causes focal degradation of gelatin films. FEBS Lett 1998;421:159–64.
32. Ohtsuka T, Shiomi T, Shimoda M, et al. ADAM28 is overexpressed in human non-small cell lung carcinomas and correlates with cell proliferation and lymph node metastasis. Int J Cancer 2006;118:263–73.
33. Fourie AM, Coles F, Moreno V, Karlsson L. Catalytic activity of ADAM8, ADAM15, and MDC-L (ADAM28) on synthetic peptide substrates and in ectodomain cleavage of CD23. J Biol Chem 2002;278: 30469–77.
34. Sung SY, Kubo H, Shigemura K, et al. Oxidative stress induces ADAM9 protein expression in human prostate cancer cells. Cancer Res 2006;66:9519–26.
35. O-Charoenrat P, Rhys-Evans PH, Eccles SA. Expression of matrix metalloproteinases and their inhibitors correlates with invasion and metastasis in squamous cell carcinoma of the head and neck. Arch Otolaryngol Head Neck Surg 2001;127:813–20.
36. Johansson N, Airola K, Grénman R, Kariniemi AL, Saarialho-Kere U, Kähäri VM. Expression of collagenase-3 (matrix metalloproteinase-13) in squamous cell carcinomas of the head and neck. Am J Pathol 1997;151:499–508.
37. Yoshizaki T, Sato H, Maruyama Y, et al. Increased expression of membrane type 1-matrix metalloproteinase in head and neck carcinoma. Cancer 1997;79:139–44.
38. Rosenthal EL, McCrory A, Talbert M, Carroll W, Magnuson JS, Peters GE. Expression of proteolytic enzymes in head and neck cancer-associated fibroblasts. Arch Otolaryngol Head Neck Surg 2004;130: 943–7.
39. Katayama A, Bandoh N, Kishibe K, et al. Expressions of matrix metalloproteinases in early-stage oral squamous cell carcinoma as predictive indicators for tumor metastases and prognosis. Clin Cancer Res 2004;10:634–40.
40. Groft LL, Muzik H, Rewcastle NB, et al. Differential expression and localization of TIMP-1 and TIMP-4 in human gliomas. Br J Cancer 2001;85:55–63.
41. Mitsui Y, Mochizuki S, Kodama T, et al. ADAM28 is overexpressed in human breast carcinomas: implications for carcinoma cell proliferation through cleavage of insulin-like growth factor binding protein-3. Cancer Res 2006;66:9913–20.
42. Rocks N, Paulissen G, El Hour M, et al. Emerging roles of ADAM and ADAMTS metalloproteinases in cancer. Biochimie 2008;90:369–79.
43. Vazquez F, Hastings G, Ortega MA, et al. METH-1, a human ortholog of ADAMTS-1, and METH-2 are members of a new family of proteins with angio-inhibitory activity. J Biol Chem 1999;274:23349–57.
44. Liu YJ, Xu Y, Yu Q. Full-length ADAMTS-1 and the ADAMTS-1 fragments display pro- and antimetastatic activity, respectively. Oncogene 2006;25:2452–67.
45. Porter S, Span PN, Sweep FC, et al. ADAMTS8 and ADAMTS15 expression predicts survival in human breast carcinoma. Int J Cancer 2006;118:1241–7.
46. Viloria CG, Obaya AJ, Moncada-Pazos A, et al. Genetic inactivation of ADAMTS15 metalloprotease in human colorectal cancer. Cancer Res 2009;69:4926–34.
47. Lo PH, Leung AC, Kwok CY, et al. Identification of a tumor suppressive critical region mapping to 3p14.2 in esophageal squamous cell carcinoma and studies of a candidate tumor suppressor gene, ADAMTS9. Oncogene 2007;26:148–57.
48. Demircan K, Gunduz E, Gunduz M, et al. Increased mRNA expression of ADAMTS metalloproteinases in metastatic foci of head and neck cancer. Head Neck 2009;31:793–801.